

Particle production as a function of underlying-event activity and search
for jet-like modifications in pp, p–Pb, and Pb–Pb collisions at
 $\sqrt{s_{\text{NN}}} = 5.02$ TeV with ALICE*

ANTONIO ORTIZ, FOR THE ALICE COLLABORATION

CERN, 1211 Geneva 23, Switzerland
UNAM, Apartado Postal 70-543, Ciudad de México 04510, México

Received July 22, 2022

The similarity between small- and large-collision systems is explored using the charged-particle multiplicity in the transverse region, N_{ch}^{T} , which is sensitive to the underlying event. Measurements of charged-particle production as a function of N_{ch}^{T} in pp, p–Pb and Pb–Pb collisions at $\sqrt{s_{\text{NN}}} = 5.02$ TeV in the toward, away and transverse regions are discussed. These three regions are defined relative to the track with the largest transverse momentum in the event ($p_{\text{T}}^{\text{trig}}$). The activity in the transverse region is subtracted from the activity in the toward and the away regions to search for jet-like modifications in small-collision systems. The jet-like signals are studied both as a function of N_{ch}^{T} and $p_{\text{T}}^{\text{trig}}$. Results are compared with two general purpose Monte Carlo event generators: PYTHIA 8 and EPOS LHC.

1. Introduction

In models incorporating multi-parton interactions (MPI), particles produced in the hard scattering (jet) are accompanied by particles from additional parton-parton interactions, as well as from the proton break-up [1]. This component of the collision makes up the underlying event (UE). The traditional UE analysis focuses on the study of particles in three topological regions depending on their azimuthal angle relative to the leading particle ($|\Delta\varphi| = |\varphi - \varphi^{\text{trig}}|$), which is the one with the highest transverse momentum in the event ($p_{\text{T}}^{\text{trig}}$). The toward region ($|\Delta\varphi| < \pi/3$ rad) contains the primary jet and UE, while the away region ($\pi/3$ rad $< |\Delta\varphi| < 2\pi/3$ rad) contains the fragments of the recoil jet and UE. In contrast, the transverse region ($|\Delta\varphi| > 2\pi/3$ rad) is dominated by the UE dynamics, but it also includes contributions from initial- and final-state radiation [2]. High-energy pp and p–Pb collisions (small-collision systems) unveiled remarkable similarities with heavy-ion collisions like collectivity, and strangeness enhancement. In heavy-ion collisions such effects are attributed to the formation of the strongly-interacting quark-gluon plasma (sQGP) [3]. Whether or not a small drop of sQGP is formed in pp and p–Pb collisions, is still a matter of debate, in particular, because jet quenching signals have not been observed so far in small-collision systems. This work discusses new results aiming at understanding small-collision systems using UE-inspired techniques [4, 5], with special emphasis on quantities which by construction are expected to be sensitive to jet quenching.

In the first part of the analysis, the average charged-particle multiplicity density (number density) in each topological region are studied as a function of the transverse momentum of the leading particle. Measurements from pp and p–Pb collisions at $\sqrt{s_{\text{NN}}} = 5.02$ TeV are reported. In the second part of the analysis, the high- p_{T} particle production in pp, p–Pb and Pb–Pb collisions at $\sqrt{s_{\text{NN}}} = 5.02$ TeV are measured as a function of the average multiplicity in the transverse region (N_{ch}^{T}). In this way the jet contribution is explicitly excluded from the multiplicity estimator, thus reducing the selection biases [6, 7]. The high- p_{T} yield in the toward and away regions after subtracting the underlying-event contribution are reported for different multiplicity classes. The multiplicity dependent yields in the jet-like signals are compared with analogous measurements in minimum-bias (MB) pp collisions. This allows to search for modifications of particle production in the jet-like signals in events with large underlying-event activity.

* Presented at the XXIXth International Conference on Ultra-relativistic Nucleus-Nucleus Collisions

2. Experimental setup and data analysis

This analysis is based on data recorded by ALICE during the pp, p–Pb, and Pb–Pb runs at $\sqrt{s_{\text{NN}}} = 5.02$ TeV. The V0 detector, and the Silicon Pixel Detector (SPD) are used for triggering and background rejection. The V0 consists of two arrays of scintillating tiles placed on each side of the interaction point covering the pseudorapidity intervals of $2.8 < \eta < 5.1$ (V0A) and $-3.7 < \eta < -1.7$ (V0C). The data were collected using a MB trigger, which required a signal in both V0A and V0C detectors. A criterion based on the offline reconstruction of multiple primary vertices in the SPD is applied to eliminate the pileup contamination. For the multiplicity dependent studies in pp and Pb–Pb collisions, the sample is subdivided into different multiplicity classes based on the total charge deposited in both V0 sub-detectors (V0M amplitude). For p–Pb collisions, the sample is subdivided based on the total charge deposited in the V0A sub-detector (V0A amplitude). The V0A amplitude selection has a small multiplicity fluctuation bias due to the enhanced contribution from the Pb-fragmentation region.

The p_{T} spectra are measured in the central barrel with the Inner Tracking System and the Time Projection Chamber following the standard procedure of the ALICE collaboration [8]. Tracks are selected in the kinematic ranges $p_{\text{T}} > 0.5$ GeV/ c and $|\eta| < 0.8$. The raw yields as a function of $p_{\text{T}}^{\text{trig}}$ or the activity in the V0 detector are corrected for efficiency and contamination from secondary particles. The efficiency correction is calculated from Monte Carlo simulations with GEANT3 [9] transport code, which made use of PYTHIA 8 (Monash) [10], EPOS-LHC [11] and HIJING [12] event generators for pp, p–Pb and Pb–Pb collisions, respectively. Since the event generators do not reproduce the relative abundances of different particle species in the real data, the efficiency obtained from the simulations is re-weighted considering the particle composition from data [8]. A multi-component template fit based on the distance-of-closest-approach distributions from the simulation is used for the estimation of secondary contamination [8]. Another correction which is relevant for $p_{\text{T}}^{\text{trig}} < 5$ GeV/ c is the leading track misidentification correction. In short, the leading particle may not be detected due to finite acceptance and efficiency of the detection apparatus, and a lower p_{T} track enters the analysis instead. If the misidentified leading particle has a different p_{T} but roughly the same direction as the true leading particle, this leads to a shift in $p_{\text{T}}^{\text{trig}}$. On the other hand, if the misidentified leading particle has a significantly different direction than the true one, this will cause a rotation of the event topology and a bias on the UE observables. The data are corrected for these effects using a data-driven procedure [4].

The main sources of systematic uncertainties include: 1) track selection criteria, 2) imperfect simulation of the detector response, 3) secondary particle contamination, 4) leading track misidentification, and 5) correction method (Monte Carlo non closure). For the estimation of the total systematic uncertainty, all the contributions were summed in quadrature.

3. Results and discussion

Figure 1 shows the number density as a function of $p_{\text{T}}^{\text{trig}}$ measured in pp and p–Pb collisions. Results are presented for the toward, transverse, and away regions. The $p_{\text{T}}^{\text{trig}}$ dependence in all regions is similar for both collision systems. For $p_{\text{T}}^{\text{trig}}$ below 5 GeV/ c the number densities exhibit a steep rise with increasing $p_{\text{T}}^{\text{trig}}$. For higher $p_{\text{T}}^{\text{trig}}$ the increases are less steep. The effect is more pronounced for the transverse region, where the number density is almost independent of $p_{\text{T}}^{\text{trig}}$. This saturation is expected in models that include the concept of impact parameter such that the requirement of the presence of a high- p_{T} particle in a pp collision biases the selection of collisions towards those with a small impact parameter [13]. The remarkable similarity between pp and p–Pb collisions indicates a similar bias in the p–Pb impact parameter, and to some extent, in the nucleon-nucleon impact parameter [14]. On the other hand, the rise of the number density observed for the toward and away regions is due to the contribution from the jet fragments. However, for these two topological regions the number densities increase faster with $p_{\text{T}}^{\text{trig}}$ in pp collisions than in p–Pb collisions. This effect is due to a larger contribution from UE to the toward and away regions in p–Pb collisions compared to pp collisions, which is expected given that in p–Pb collisions more than one

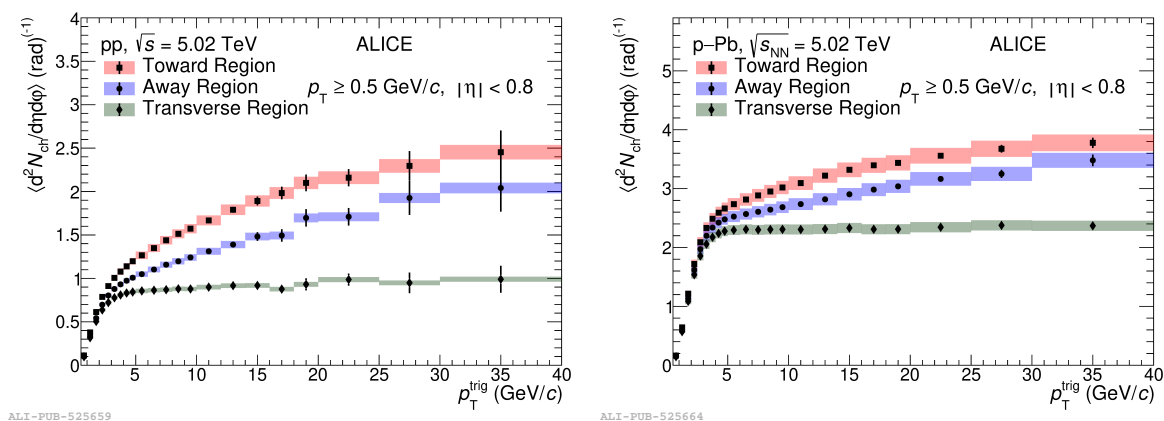


Fig. 1: Number density as a function of p_T^{trig} measured in pp (left) and p-Pb collisions (right) at $\sqrt{s_{\text{NN}}} = 5.02$ TeV. Results for the toward, transverse, and away regions are displayed. The boxes and the error bars represent the systematic and statistical uncertainties, respectively.

nucleon-nucleon interaction can occur.

As discussed earlier, requiring a high- p_T particle makes an indirect selection of collisions with small impact parameters possible. Thus, it is interesting to compare the particle produced in the hard scattering in pp and p-Pb collisions for similar p_T^{trig} intervals. In this way, given that the UE activity is 2.4 times larger in p-Pb than in pp collisions, one can search for possible jet-like modifications in p-Pb collisions. In order to increase the sensitivity to the particles produced in the hard scattering, jet-like signals are obtained from the number density in the toward and away regions after subtracting the number density in the transverse region. Figure 2 shows the jet-like contribution to the number density in the toward and away regions as a function of p_T^{trig} for pp and p-Pb collisions at $\sqrt{s_{\text{NN}}} = 5.02$ TeV. The number densities in the jet-like signals rise with increasing p_T^{trig} in the entire range of the measurement. At high p_T^{trig} (> 10 GeV/c), the number density exhibits a remarkable similarity between pp and p-Pb collisions. Within 10%, both PYTHIA 8 Angantyr [15] and EPOS LHC reproduce this feature. This is consistent with the absence of medium effects in minimum-bias p-Pb collisions at high p_T^{trig} . At lower p_T^{trig} , the models overestimate the number density in p-Pb collisions. The disagreement is more remarkable for EPOS LHC than for PYTHIA 8 Angantyr. The number density in pp collisions scaled to that in p-Pb collisions is smaller than unity, reaching a minimum of ≈ 0.8 at $p_T^{\text{trig}} \approx 3$ GeV/c. This behaviour is not reproduced by PYTHIA 8 Angantyr. In contrast, EPOS LHC exhibits a similar pattern, but the size of the effect is much larger than in data. The main difference between PYTHIA 8 Angantyr and EPOS LHC is that EPOS LHC incorporates collective flow, which is expected to give an effect in the p_T^{trig} interval where the differences between measurements in pp and p-Pb collisions are observed. Moreover, the Angantyr model in PYTHIA 8 extrapolates the dynamics from pp collisions to p-Pb and Pb-Pb collisions, generalising the formalism adopted for pp collisions by including a description of the nucleon positions within the colliding nuclei and utilising the Glauber model to calculate the number of interacting nucleons and binary nucleon-nucleon collisions.

To further investigate the possible modification of the particles produced in the hard scattering using pp and p-Pb data, only collisions containing a leading track transverse momentum within $8 < p_T^{\text{trig}} < 15$ GeV/c are considered. Moreover, small-collision systems are compared with Pb-Pb collisions at the same centre-of-mass energy per nucleon pair, where there is enough evidence of medium jet modifications due to the presence of sQGP. The high- p_T yields ($4 < p_T < 6$ GeV/c) in the toward (Y^t) and away (Y^a) regions obtained after the subtraction of the high- p_T yield in the transverse region (Y^T) are measured. The subtracted yields ($Y^{\text{st,sa}}$) are further normalised to those measured in MB pp collisions. With these quantities the $I_X^{\text{t,a}}$ factors are defined as follows:

$$I_X^{\text{t,a}} \equiv (Y_X^{\text{t,a}} - Y_X^{\text{T}}) / (Y_{\text{pp,MB}}^{\text{t,a}} - Y_{\text{pp,MB}}^{\text{T}}) = Y_X^{\text{st,sa}} / Y_{\text{pp,MB}}^{\text{st,sa}}, \quad (1)$$

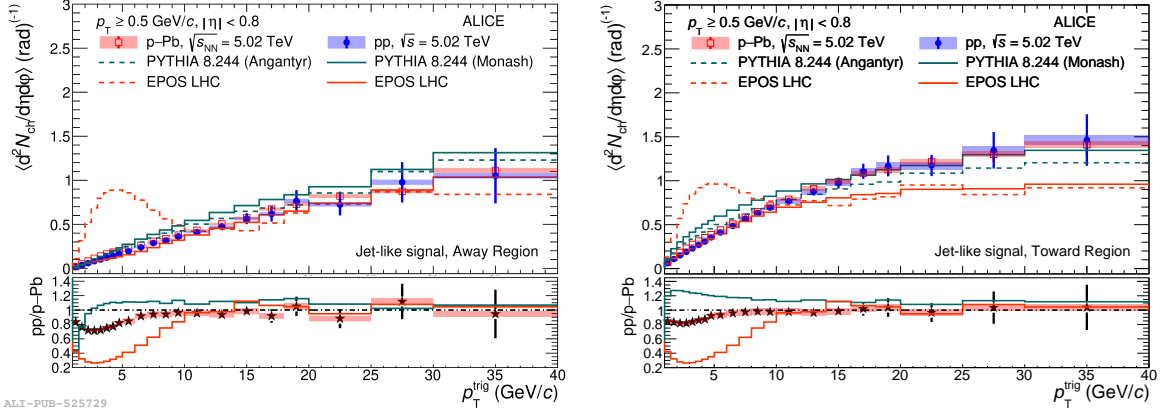


Fig. 2: Number density as a function of p_T^{trig} in pp and p-Pb collisions at $\sqrt{s_{\text{NN}}} = 5.02$ TeV. Results for the jet-like signals in the away (left) and toward (right) regions are shown. The pp results scaled to the p-Pb ones are displayed in the bottom panel.

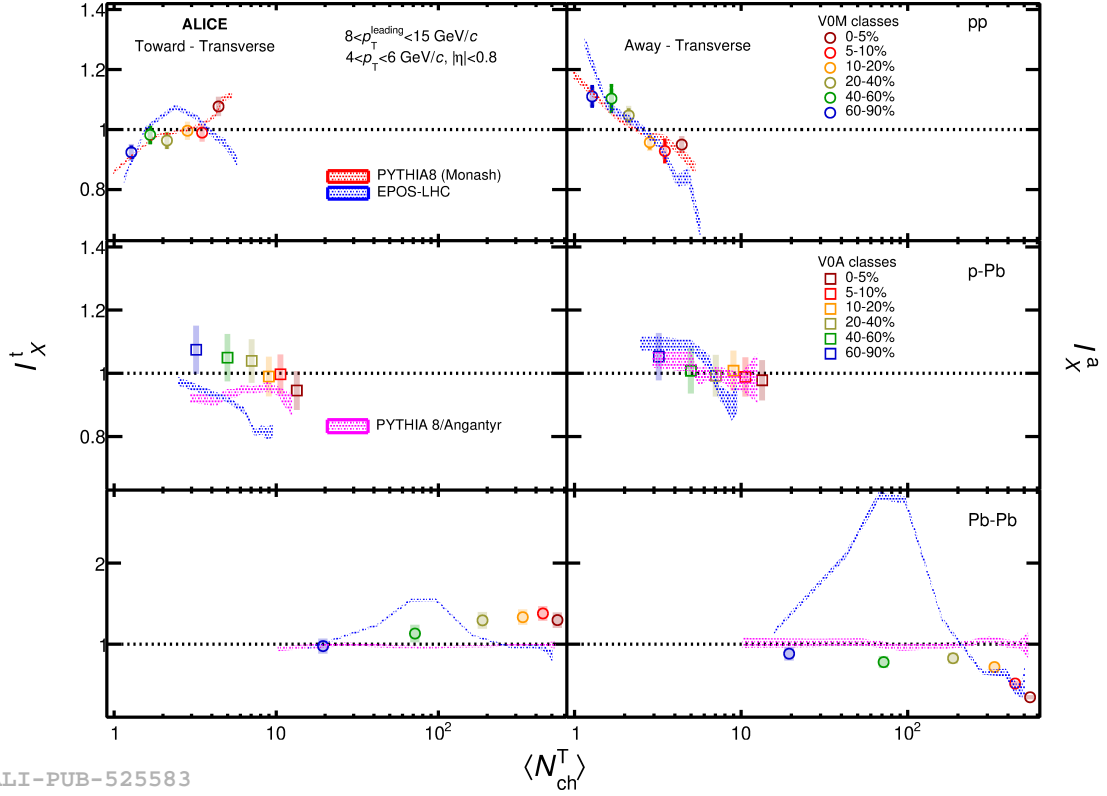
where X indicates the collision system and the event multiplicity class. In the absence of medium effects or selection biases, this quantity is expected to be consistent with unity.

Figure 3 shows $I_X^{t,a}$ as a function of $\langle N_{\text{ch}}^T \rangle$ for pp, p-Pb and Pb-Pb collisions. Data are compared with PYTHIA 8 and EPOS LHC. As discussed earlier the events were classified in terms of the activity in the V0 detector. This reduces the presence of particles from hard Bremsstrahlung gluons that can contribute to the transverse region [16]. Within uncertainties, the $I_X^{t,a}$ values are close to unity for all the multiplicity classes measured in pp collisions. The small multiplicity dependence observed in pp collisions is due to selection biases. Within uncertainties, the effect is well reproduced by PYTHIA 8, which does not incorporate any jet quenching mechanism. The origin of this small effect in high $\langle N_{\text{ch}}^T \rangle$ collisions is related to a remaining bias towards harder fragmentation and more activity from initial and final state radiation. The results indicate that effects induced by possible energy loss in pp collisions are not observed within uncertainties in the multiplicity and transverse momentum ranges reported in this work.

For p-Pb collisions, within uncertainties, the $I_X^{t,a}$ values are close to unity for all the multiplicity classes. The data are compared to PYTHIA 8 Angantyr [15] and EPOS-LHC predictions. The Angantyr model predicts the I_X^a factor to be consistent with unity, and I_X^t slightly below unity. On the other hand, EPOS-LHC does not describe neither the magnitude nor the trend of the multiplicity dependence of the measured ratio in the toward region, I_X^t . However, the model is in reasonable agreement with data in the away region. Data from p-Pb collisions indicate the absence of medium effects in both the toward and away regions within the multiplicity and transverse momentum intervals reported in this work.

By contrast, for Pb-Pb collisions the $I_X^{t,a}$ values are compatible with unity for peripheral collisions, and show a gradual increase (reduction) with the increase in multiplicity for the toward (away) region. The behaviour is the same even considering the modulation of the underlying event by elliptic flow (v_2). The interpretation of the results is similar to that reported in [17]. On the one hand, the suppression in the away region is expected from the strong in-medium energy loss; on the other hand, the enhancement observed in the toward region is also subject to medium effects. The ratio is sensitive to a) a possible change of the fragmentation functions, b) a possible modification of the quark-to-gluon jet ratio in the final state due to different coupling with the medium, and c) a possible bias on the parton spectrum due to trigger particle selection. It is likely that all three effects play a role [17]. Regarding the model comparisons, PYTHIA 8 Angantyr, which does not include jet quenching effects, predicts $I_X^{t,a}$ values consistent with unity for all the multiplicity classes in Pb-Pb collisions. In EPOS-LHC, a certain p_T cutoff is defined in such a way that, above this cutoff, a particle loses part of its momentum in the core but survives as an independent particle produced by a flux tube. Soft particles, which are below the p_T cutoff, get completely absorbed and form the core. This sort of energy loss mechanism implemented in EPOS-LHC depends on the system

size [11, 18, 19]. With these implementations, EPOS-LHC predicts a significant enhancement of $I_X^{t,a}$ for low $\langle N_{\text{ch}}^T \rangle$ ranges and deviates significantly from the experimental results. However, it reasonably describes I_X^a at high multiplicities.



ALI-PUB-525583

Fig. 3: Comparison of the measured I_X^t (left) and I_X^a (right) in $4 < p_T < 6$ GeV/c with model predictions. The results are shown as a function of $\langle N_{\text{ch}}^T \rangle$ for different multiplicity classes in pp (top panel), p-Pb (middle panel) and Pb-Pb (bottom panel) collisions at $\sqrt{s_{\text{NN}}} = 5.02$ TeV. The red and magenta lines show the PYTHIA 8 (Monash) [10] and PYTHIA 8 Angantyr [10] predictions, respectively. The blue lines show the EPOS-LHC [11] results. The statistical and systematic uncertainties are shown by bars and boxes, respectively.

4. Conclusions

For the first time the properties of the underlying event are measured in collisions involving heavy ions. The charged-particle densities as a function of p_T^{trig} exhibit a saturation at $p_T^{\text{trig}} \approx 5$ GeV/c in the transverse region for both pp and p-Pb collisions at $\sqrt{s_{\text{NN}}} = 5.02$ TeV. In models like PYTHIA 8 this effect is due to a bias towards collisions with small impact parameter. The results for the toward and away regions are also remarkably similar in pp and p-Pb collisions. In order to investigate the presence of medium effects at high p_T in jet-like signals, the charged-particle density in the toward and away regions are studied after subtracting the number density in the transverse region. For $p_T^{\text{trig}} > 10$ GeV/c the number densities are compatible in pp and p-Pb collisions. An additional measurement that considers collisions containing a leading particle within $8 < p_T^{\text{trig}} < 15$ GeV/c is also reported. The high- p_T yields ($4 < p_T < 6$ GeV/c) are measured in different multiplicity classes for pp, p-Pb and Pb-Pb collisions at $\sqrt{s_{\text{NN}}} = 5.02$ TeV, the yields are compared with analogous measurements in minimum-bias pp collisions. While the data from Pb-Pb collisions are in agreement with expectations from parton energy loss due to the presence of a hot and dense medium, pp and p-Pb data do not show any hint of medium effects in the multiplicity and transverse momentum ranges which are reported.

5. Acknowledgement

This work has been supported by CONACyT under the Grants CB No. A1-S-22917 and CF No. 2042, as well as by UNAM under the program PASPA-DGAPA.

REFERENCES

- [1] T. Sjöstrand and M. van Zijl, “A Multiple Interaction Model for the Event Structure in Hadron Collisions,” *Phys. Rev. D* **36** (1987) 2019.
- [2] G. Bencedi, A. Ortiz, and A. Paz, “Disentangling the hard gluon bremsstrahlung effects from the relative transverse activity classifier in pp collisions,” *Phys. Rev. D* **104** no. 1, (2021) 016017, [arXiv:2105.04838 \[hep-ph\]](#).
- [3] Busza, Wit and Rajagopal, Krishna and van der Schee, Wilke, “Heavy Ion Collisions: The Big Picture, and the Big Questions,” *Ann. Rev. Nucl. Part. Sci.* **68** (2018) 339–376, [arXiv:1802.04801 \[hep-ph\]](#).
- [4] **ALICE** Collaboration, “Underlying-event properties in pp and p–Pb collisions at $\sqrt{s_{NN}} = 5.02$ TeV,” [arXiv:2204.10389 \[nucl-ex\]](#).
- [5] **ALICE** Collaboration, “Study of charged particle production at high p_T using event topology in pp, p–Pb and Pb–Pb collisions at $\sqrt{s_{NN}} = 5.02$ TeV” [arXiv:2204.10157 \[nucl-ex\]](#).
- [6] T. Martin, P. Skands, and S. Farrington, “Probing Collective Effects in Hadronisation with the Extremes of the Underlying Event,” *Eur. Phys. J. C* **76** no. 5, (2016) 299, [arXiv:1603.05298 \[hep-ph\]](#).
- [7] S. G. Weber, A. Dubla, A. Andronic, and A. Morsch, “Elucidating the multiplicity dependence of J/ψ production in proton–proton collisions with PYTHIA8,” *Eur. Phys. J. C* **79** no. 1, (2019) 36, [arXiv:1811.07744 \[nucl-th\]](#).
- [8] **ALICE** Collaboration, S. Acharya *et al.*, “Transverse momentum spectra and nuclear modification factors of charged particles in pp, p-Pb and Pb-Pb collisions at the LHC,” *JHEP* **11** (2018) 013, [arXiv:1802.09145 \[nucl-ex\]](#).
- [9] R. Brun, F. Bruyant, F. Carminati, S. Giani, M. Maire, A. McPherson, G. Patrick, and L. Urban, *GEANT: Detector Description and Simulation Tool; Oct 1994*. CERN Program Library. CERN, Geneva, 1993. <https://cds.cern.ch/record/1082634>. Long Writeup W5013.
- [10] P. Skands, S. Carrazza, and J. Rojo, “Tuning PYTHIA 8.1: the Monash 2013 Tune,” *Eur. Phys. J. C* **74** no. 8, (2014) 3024, [arXiv:1404.5630 \[hep-ph\]](#).
- [11] T. Pierog, I. Karpenko, J. M. Katzy, E. Yatsenko, and K. Werner, “EPOS LHC: Test of collective hadronization with data measured at the CERN Large Hadron Collider,” *Phys. Rev. C* **92** no. 3, (2015) 034906, [arXiv:1306.0121 \[hep-ph\]](#).
- [12] W.-T. Deng, X.-N. Wang, and R. Xu, “Hadron production in p+p, p+Pb, and Pb+Pb collisions with the HIJING 2.0 model at energies available at the CERN Large Hadron Collider,” *Phys. Rev. C* **83** (2011) 014915, [arXiv:1008.1841 \[hep-ph\]](#).
- [13] M. Strikman, “Transverse Nucleon Structure and Multiparton Interactions,” *Acta Phys. Polon. B* **42** (2011) 2607–2630, [arXiv:1112.3834 \[hep-ph\]](#).
- [14] **ALICE** Collaboration, J. Adam *et al.*, “Centrality dependence of particle production in p-Pb collisions at $\sqrt{s_{NN}} = 5.02$ TeV,” *Phys. Rev. C* **91** no. 6, (2015) 064905, [arXiv:1412.6828 \[nucl-ex\]](#).
- [15] C. Bierlich, G. Gustafson, L. Lönnblad, and H. Shah, “The Angantyr model for Heavy-Ion Collisions in PYTHIA8,” *JHEP* **10** (2018) 134, [arXiv:1806.10820 \[hep-ph\]](#).
- [16] G. Bencedi, A. Ortiz, and S. Tripathy, “Apparent modification of the jet-like yield in proton-proton collisions with large underlying event,” *J. Phys. G* **48** no. 1, (2020) 015007, [arXiv:2007.03857 \[hep-ph\]](#).
- [17] **ALICE** Collaboration, K. Aamodt *et al.*, “Particle-yield modification in jet-like azimuthal di-hadron correlations in Pb-Pb collisions at $\sqrt{s_{NN}} = 2.76$ TeV,” *Phys. Rev. Lett.* **108** (2012) 092301, [arXiv:1110.0121 \[nucl-ex\]](#).
- [18] R. Baier, Y. L. Dokshitzer, A. H. Mueller, S. Peigne, and D. Schiff, “Radiative energy loss of high-energy quarks and gluons in a finite volume quark - gluon plasma,” *Nucl. Phys. B* **483** (1997) 291–320, [arXiv:hep-ph/9607355](#).
- [19] S. Peigne, “Collisional Energy Loss of a Fast Parton in a QGP,” *AIP Conf. Proc.* **1038** no. 1, (2008) 139–148, [arXiv:0806.0242 \[hep-ph\]](#).